Self-assembled hyaluronate/protamine polyelectrolyte nanoplexes: Synthesis, stability, biocompatibility and potential use as peptide carriers

Anita Umerska [a)], Krzysztof J. Paluch [a)], Maria-Jose Santos Martinez [a), b)], Owen I. Corrigan [a)], Carlos Medina [a)], Lidia Tajber [a)*]

a) School of Pharmacy and Pharmaceutical Sciences & Trinity Biomedical Sciences Institute, Trinity College Dublin, Dublin 2, Ireland.

b) School of Medicine, Trinity College Dublin, Dublin 2, Ireland.

*To whom correspondence should be addressed: lidia.tajber@tcd.ie, Phone: 00353 1 896 2787, Fax: 00353 1 896 2810

KEYWORDS: hyaluronic acid, protamine, calcitonin, nanoparticles, polyelectrolyte complex, Caco 2- cells

Manuscript number: 13-519-RRR

Received: June 17, 2013; 1st Revision received: September 17, 2013; 2nd Revision received: November 3, 2013; Accepted: November 26, 2013

Abstract

This work investigates a new type of polyelectrolyte complex nanocarrier composed of hyaluronic acid (HA) and protamine (PROT). Small (approximately 60 nm) and negatively charged nanoparticles (NPs) with a polydispersity index of less than 0.2 were obtained with properties that were dependent on the mixing ratio, concentration of polyelectrolytes and molecular weight of HA. Salmon calcitonin (sCT) was efficiently (up to 100%) associated with the NPs, and the drug loading (9.6-39% w/w) was notably high, possibly due to an interaction between HA and sCT. The NPs released ~70-80% of the sCT after 24 hours, with the estimated total amount of released sCT depending on the amount of HA and PROT present in the NPs. The isoelectric point of the NPs was close to pH 2, and the negative surface charge was maintained above this pH. The HA/PROT nanoplexes protected the sCT from enzymatic degradation and showed low toxicity to intestinal epithelial cells, and thus may be a promising oral delivery system for peptides.

1. Introduction

It has been demonstrated that it is possible to form HA-based polyelectrolyte-complex NPs, but most of the work conducted thus far has focused on HA/chitosan NPs[1,2,3,4]. However, as a polyanion, HA has the ability to form polyelectrolyte complexes with other polycations. Among these materials, polypeptides and proteins are of great interest because of their biodegradability and biocompatibility. For instance, complexes of HA based on electrostatic attraction with poly-L-lysine[5] and lysozyme[6,7] have been formulated and examined. Reports have been published on complexation of HA with poly-arginine, resulting in the formation of polyelectrolyte-complex NPs.[8,9] Both research groups obtained small NPs with sizes of approximately 90-170 nm that were positively[8,9] or negatively charged.[9] Kim et al. used these NPs as carriers for delivery of siRNA.[8] Oyarzun-Ampuyero et al. successfully produced NPs via simple mixing of polycation and polyanion solutions, and no cross-linker was used.[9] Although this group indicated that incorporation of hydrophilic macromolecular drugs, e.g., peptides, into their nanocarriers may be possible, no such studies have been published thus far. Additionally, the high cost of polyarginine may be one of the disadvantages of its use in drug delivery.

Hence, another polycation is required that could be complexed to HA to produce NPs. Ideally, such a compound should be reasonably inexpensive, already well characterized and should have a history of use in pharmaceutical products, thus minimizing the need for additional biodegradability and toxicity studies. Protamine (PROT) can be considered as a promising candidate because it is a naturally occurring and strongly charged cationic protein and already used in formulations that contain insulin.[10] Additionally, PROT is used as a drug itself in applications as an antagonist for heparin. Similar to certain viral proteins that use arginine-rich sequences of amino acids to provide membrane-translocation activities, PROT consists of a mixture of positively charged proteins extracted from salmon roe and is rich in

arginine,. Indeed, Reynolds et al. showed that PROT displays membrane translocation activity, which is a desirable property for protamine-based formulations intended for use in pharmaceutical applications.[11] Moreover, protamine offers a long history of use and established biological effects and general safety in humans.[11]

Junghans et al. showed that complexation to protamine protected oligonucleotides from enzymatic degradation and increased their cellular uptake.[12] Additionally, PROT has been shown to form polyelectrolyte complexes NPs with heparin and with a glycosaminoglycan such as HA but with a higher charge density. Mori et al. succeeded in producing polyelectrolyte-complex micro- and nanoparticles containing heparin and PROT as a carrier for fibroblast growth factor-2 (FGF-2).[13] The NPs appeared to maintain the mitogenic activity of FGF-2 and protect the peptide from inactivation by heat.

Both HA and PROT have been combined in a sustained release delivery system. Mini-pellets composed of HA/recombinant human interleukin 11 (rhIL11) and HA/PROT/rhIL11 were observed to enhance the *in vivo* efficacy of the cytokine, which was attributed to the interactions between HA and rhIL11.[14] A longer plasma residence time was measured for rhIL11 released from HA/PROT pellets, which was accompanied by an increase in pharmacologic efficacy.[14] Mok et al., showed that a conjugate of HA and an anti-sense oligonucleotide used to form a nanocomplex with PROT was characterized by better cellular uptake compared with that of unconjugated physical complexes formed between PROT and naked oligonucleotides.[15]

We recently presented studies on the optimum formation condition and properties of crosslinker- and surfactant-free HA/chitosan NPs[4] and also showed that salmon calcitonin/HA/chitosan NPs were able to reduce experimental inflammatory arthritis.[16] Because HA and sCT produced important anti-inflammatory effects *in vitro*[16], an HA-based delivery system appears to be a particularly suitable carrier for sCT. Calcitonin is currently

recommended for short-term use in Paget's disease, acute bone loss due to sudden immobilization and hypercalcaemia caused by cancer.[17]

Considering that no nanosized drug delivery system based on HA and PROT has been reported to date, the aims of the current work were to investigate the conditions of such nanocarrier formation by adopting the previously presented manufacturing process[4], to evaluate the properties of NPs formation and to explore the ability of HA/PROT NPs to bind, release and protect sCT.

2. Materials and methods

2.1 Materials

Hyaluronic acid sodium salt (HA) from *Streptococcus equi* sp. and protamine sulfate (PROT, molecular weight of 5.1 kDa; manufacturer data) were purchased from Sigma (USA). Pepsin from porcine gastric mucosa (cat. no. P6887, 4220 IU/mg) and trypsin from bovine pancreas (cat. no. T8003, 12238 BAEE/mg) were sourced from Sigma Aldrich (Ireland). Salmon calcitonin (sCT) was obtained from PolyPeptide Laboratories (Denmark), APC annexin V and propidium iodide were obtained from BD Biosciences (USA) and CellTiter 96® Non-Radioactive Cell Proliferation Assay was purchased from Promega Corporation (USA). Other cell culture reagents were provided by Sigma Aldrich (Ireland). All other reagents, chemicals and solvents were of analytical grade.

2.2 Preparation of HA/PROT carriers and HA/PROT/sCT NPs

The HA solutions with concentrations of 0.1 or 0.2% w/v were prepared in deionized water, and HA with molecular weights of 176 kDa, 257 kDa and 590 kDa (later referred to as HA176, HA257 and HA590, respectively) were obtained via ultrasonication of native HA (2882±24.5 kDa), as previously described.[4] The PROT solutions with concentrations of 0.2-3.2 mg/ml were also prepared using deionized water.

The NP carriers (NPs without the cargo) were formed by adding 4 ml of an aqueous PROT solution to 10 ml of an HA solution at room temperature under magnetic stirring. The stirring was maintained for 10 minutes to allow stabilization of the system. A dispersion of particles was instantaneously obtained upon mixing of the polymer solutions. Because PROT solutions with different concentrations were used, the NP dispersions that were formed had different compositions of HA (equivalent to 0.71 mg/ml or 1.43 mg/ml in the final formulation) and PROT (equivalent to 0.06-0.91 mg/ml in the final formulation). The PROT weight fraction in the HA/PROT NPs was calculated as the ratio of the weight of PROT to the total weight of HA and PROT used to form a given system.

The NPs containing sCT were formed by following the above procedure with a modification for an appropriate quantity of the peptide, resulting in a final sCT concentration in the NP dispersion of 0.1 mg/ml, 0.5 mg/ml and 1.0 mg/ml (equivalent to 1.4 mg, 7.0 mg and 14.0 mg of sCT in 10 ml of HA solution, respectively) as dissolved in the HA solution prior to mixing with the PROT solution.

2.3 NPs characterization and stability

2.3.1 Transmittance measurements

The transmittance of the NP dispersions was measured using an UV-1700 PharmaSpec UV-Visible spectrophotometer (Shimadzu, Japan) at an operating wavelength of 500 nm in optically homogenous quartz cuvettes (Hellma, Germany) with a light path of 10 mm.[4]

2.3.2 Particle size and zeta potential analysis

The intensity-averaged mean particle size (hydrodynamic particle diameter) and the polydispersity index of the NPs were determined using Dynamic Light Scattering (DLS) with 173º backscatter detection. The electrophoretic mobility values measured by Laser Doppler Velocimetry (LDV) were converted to zeta potentials using the Smoluchowski equation. Both

the DLS and LDV measurements were collected on a Zetasizer Nano series Nano-ZS ZEN3600 fitted with a 633-nm laser (Malvern Instruments Ltd., UK). Samples were placed directly into the folded capillary cells without dilution. Each analysis was carried out at 25ºC with the equilibration time set to 5 minutes. The readings were repeated at least three times for each batch, and the average values of at least three batches are presented. The results obtained were corrected for the sample viscosity measured at 25±0.2ºC with a low frequency vibration viscometer (SV-10 Vibro Viscometer, A&D Company Limited, Japan).[4]

2.3.3 Transmission electron microscopy (TEM)

The TEM image collection was performed with a JEM-2100 instrument (Jeol, USA), as described previously.[4] One drop of NP suspension was deposited onto a copper grid, held for 60 seconds and the excess liquid was blotted off using filter paper. The immobilized samples were stained by deposition of one drop of 1% w/v ammonium molybdate solution for 60 seconds. The excess liquid was again blotted off using filter paper, and the grids were dried overnight for viewing with TEM. The acceleration voltage was 200 kV.

2.3.4 Scanning electron microscopy (SEM)

The SEM collection was carried out with a Supra Variable Pressure Field Emission Scanning Electron Microscope (Zeiss, Germany) equipped with a secondary electron detector at 2 kV.[18] An amount of 50 µl of liquid sample was directly placed onto an aluminum stub, dried for 24 hours at ambient temperature in a desiccator over silica gel and sputter-coated with gold under vacuum prior to analysis.

2.3.5 pH measurements

A pH meter (Orion model 520A, Thermo Scientific, USA) equipped with an Orion Ross™ 8103SC glass-body pH semi-micro electrode was used for the pH measurements. The pH meter was calibrated using standard buffer solutions (Thermo Scientific, USA) of pH 4.00, 7.00 and 10.00 (±0.01).

2.3.6 Physical stability of nanoparticles

Physical stability studies of the NPs in native and undiluted dispersions were performed in polypropylene tubes upon storage at room temperature for a period of up to 4 weeks in a dark environment. Samples from each formulation were withdrawn periodically during the studies, and the particle size, zeta potential and transmittance were measured.

2.3.7 Determination of the isoelectric point of NPs

A Zetasizer Nano series Nano-ZS ZEN3600 particle sizer fitted with a 633-nm laser together with a MPT-2 autotitrator (Malvern Instruments Ltd., UK) were used to determine the isoelectric point of the NPs.[4] Amounts of 0.25M HCl and 0.25M NaOH were used as titrants. A total of 12 ml of NP dispersion was added initially to the sample container. Each analysis was carried out at room temperature in automatic mode using the target pH tolerance of 0.2 units. Three particle size measurements and three zeta potential measurements were carried out for each pH value, and the samples were re-circulated between repeat measurements.

2.4 Salmon calcitonin (sCT) loading studies

2.4.1 Separation of non-associated sCT

Non-associated sCT was separated from the NPs using a combined ultrafiltration-centrifugation technique (Centriplus YM-50, MWCO of 50 kDa, Millipore, USA).[16] A total of 5 ml of sample was placed in the sample reservoir (donor phase) of the centrifugal filter device and centrifuged for 1 hour at 4,537 g (3,000 rpm). After centrifugation, the volume of the solution in the filtrate vial (acceptor phase) was measured, and the filtrate was assayed for sCT content via HPLC, as described below. This quantity of sCT was referred to as the non-associated sCT.

The NP suspension from the sample reservoir was standardized to 5 ml with deionized water. A total of 0.75 ml of the NP suspension from the sample reservoir was mixed with 0.75

ml of 0.1 mM NaOH (this NaOH concentration was optimized and did not cause sCT degradation) to break up the NPs and release sCT, and the mixture was centrifuged for 30 minutes at 16,060 g (13,000 rpm). The supernatant was assayed for sCT content via HPLC, and this portion of the peptide was referred to as the extracted sCT. A good mass balance of sCT was obtained if it were possible to extract more than 90% of the associated sCT. The remainder of the dispersion from the sample reservoir was analyzed for particle size, zeta potential and transmittance. The particle size, zeta potential and transmittance and the pH and viscosity of the nanoparticles before separation of the non-associated sCT were also measured.

The association efficiency (AE) and drug loading (DL) were calculated using the following equations:[1]

$$AE = \left[\frac{A-B}{A}\right] * 100\% \quad \text{(Eqn. 1)}$$

where A is the total amount (mass) of the sCT, and B is the mass of the non-associated sCT

$$DL = \left[\frac{A-B}{C}\right] * 100\% \quad \text{(Eqn. 2)}$$

where C is the total weight of all components of the NPs (the associated sCT and the mass of HA and PROT used for the preparation of NPs).

2.4.2 Release studies

Aliquots of 250 µl of NPs were added to 2.25 ml of PBS (137 mM NaCl, 2.7 mM KCl, 1.4 mM NaH_2PO_4, 1.3 mM Na_2HPO_4 adjusted to pH 7.4 with NaOH solution). The samples were incubated at 37ºC at 100 cpm in a reciprocal shaking water bath (model 25, Precision Scientific, India). After 1, 2, 4, 6 and 24 hours, 2.5 ml aliquots were withdrawn, and the released sCT was separated using the combined ultrafiltration-centrifugation technique as described above. The samples were centrifuged at 6,805 g (4,500 rpm) for 15 minutes. After centrifugation, the volume of the solution from the filtrate vial (acceptor phase) was measured, and the filtrate was assayed for sCT content via HPLC (released sCT; the HPLC

method is described below). The NP suspension from the sample reservoir was standardized to 2.5 ml with PBS and returned to the water bath to continue the release studies.[16]

The data from the release studies were fitted to the first-order equation:

$W = W_{\infty}(1 - e^{-kt})$ (Eqn. 3)

where W is the total amount of the peptide released at time t (based on cumulative release), W_{∞} is the amount of the peptide released at infinity and k is the release rate constant.[19]

2.4.3 Quantification of sCT

Analysis of sCT content was performed using an HPLC system as described previously.[16] Briefly, standard solutions of sCT (1.5–50 µg/ml) were prepared in deionized water, and 50 µl of the standard or sample was injected into the Jones Chromatography Genesis 4µ C18 150 × 4.6 mm column (Crawford Scientific Ltd, UK). A flow rate of 1 ml/min was employed using a mobile phase composed of 0.116% w/v NaCl, 0.032% v/v TFA, and 34% v/v acetonitrile. The UV detection was carried out at 215 nm. The sCT peak had a retention time of ~5 min. Data collection and integration were accomplished using CLASS-VP software (version 6.10, Shimadzu, Japan).

2.5 Enzymatic degradation of sCT

Stability analysis of sCT in the presence of pepsin and trypsin was carried out using a HA/PROT NP system with an MMR of 6.3 and an sCT loading of 0.2 mg/ml as well as 0.2 mg/ml sCT solution (made up in 0.9% NaCl). A pepsin stock solution with a concentration of 20,000 IU/ml was prepared in pepsin-free simulated gastric fluid (SGF, HCl solution with pH 1.2 containing 0.2% w/v NaCl, Ph. Eur. 7th edition[20]). The trypsin stock solution (2,900 BAEE/ml) was prepared in phosphate buffered saline (PBS, pH 7.4).

For the experiments with pepsin, 2.5 ml of NPs-sCT or sCT solution was mixed with 2.5 ml of SGF and 50 µl of pepsin stock solution such that the initial concentrations of sCT and pepsin were 0.1 mg/ml and 200 IU/ml, respectively. The control sample was prepared

with 2.5 ml of NPs-sCT or sCT solution, 2.5 ml of SGF and 50 µl of SGF (pepsin-free). For the experiments with trypsin, 2.5 ml of NPs-sCT or sCT solution was mixed with 2.5 ml of PBS and 12 µl of trypsin stock solution such that the initial concentrations of sCT and trypsin were 0.1 mg/ml and 7 BAEE/ml, respectively. The control sample was prepared with 2.5 ml of NPs-sCT or sCT solution, 2.5 ml of PBS and 12 µl of PBS. All samples, controls and enzyme-containing mixtures were incubated at 37°C.

At given time intervals, 0.7 ml of the sample was withdrawn from each mix, and the enzymatic reaction was stopped by addition of 0.1 ml of 1M NaOH (to samples with pepsin and controls for experiments with pepsin) or 0.1 ml of 1M HCl (to samples with trypsin and controls for experiments with trypsin). The 0.8-ml aliquots were centrifuged at 16,060 g (13,000 rpm) for 5 min at 4°C, and the amount of sCT remaining in the supernatant was determined via HPLC, as described in Section 2.4.3.

2.6 Cell culture and *in vitro* cytotoxicity studies

Human colon adenocarcinoma cells (Caco-2) were obtained from the European Collection of Cell Cultures. Cells were cultured as a monolayer in Eagle's Minimal Essential Medium (MEM) supplemented with 20% fetal bovine serum (FBS), penicillin (0.006 mg/ml), streptomycin (0.01 mg/ml), gentamicin (0.005 mg/ml), sodium bicarbonate (2.2 g/l) and sodium pyruvate (0.11 g/l) in a 5% CO_2 and 37ºC humidified atmosphere (CO_2 incubator series 8000DH, Thermo Scientific, USA). Cells were supplied with fresh medium every second day and split after detachment with EDTA-trypsin twice a week. For experimental purposes, the passage number range was maintained between 20 and 30.

2.6.1 MTS assay

The Caco-2 cells were seeded into flat-bottom 96-well plates in 100 µl of MEM containing 20% FBS at a density of 25,000 cells per well and incubated at 37ºC for one day. The medium was replaced with 100 µl of the sample dispersed or dissolved in serum-free

media. After 72 hours of incubation, the supernatant was removed from the wells and replaced with serum-free media. An amount of 20 µl of MTS reagent prepared according to the manufacturer protocol was added into each well; in the case of the positive control (0% viability), the media was replaced with a 10% SDS solution in serum-free media 30 min before the addition of MTS reagent. After 4 hours, the UV absorbance of the formazan product was measured spectrophotometrically (FLUOstar Optima microplate reader, BMG Labtech, Germany) at 492 nm. The positive control was treated as a blank, and its absorbance was subtracted from each reading. The cell viability was expressed as the ratio of the absorbance reading of the cells treated with different samples and that of the negative control (cells treated with serum-free MEM), which was assumed to have 100% cell viability. The IC50 values (concentrations required to reduce the viability of cells by 50% compared with the control cells) were calculated by fitting the experimental points to the Hill equation.[21]

2.6.2 Flow cytometry

The Caco-2 cells were incubated with 3 ml of sample for 72 h. Next, the supernatant was removed, and the cells were harvested with 1 ml of trypsin/EDTA. After neutralization with 10 ml of MEM with 10% FBS, the cells were combined with the previous supernatant and centrifuged (300 g, 5 minutes). The supernatant from the centrifugation was discarded, and the cells were washed with binding buffer (0.14M NaCl, 0.0025M $CaCl_2$ and 0.01M HEPES, pH 7.4). A total of 20 µl of the cell suspension was stained with 5 µl of APC-Annexin V and 5 µl of propidium iodide (PI), diluted with 70 µl of binding buffer and incubated in the dark at room temperature for 15 minutes. Next, the cell suspension was further diluted with binding buffer, transferred to a flat-bottom 96-well plate and subjected to flow cytometry analysis. All analyses were performed using a BD FACSArray™ bioanalyser (Becton Dickinson, UK). The instrument was set up to measure the size (forward scatter), granularity (side scatter) and cell fluorescence. Antibody binding was measured by analyzing

individual cells for fluorescence. The mean fluorescence intensity was determined after correction for cell auto-fluorescence, and fluorescence histograms were obtained for 10,000 individual events. Data were analyzed using the BD FACSArray^{TM} system software and expressed as a percentage of control fluorescence in arbitrary units.

2.7 Statistical analysis

The statistical significance of the differences between samples was determined using one-way analysis of variance (ANOVA) followed by the post-hoc Tukey's test using Minitab software (version 14, Minitab, USA). Differences were considered significant at $p<0.05$.

3.Results and discussion

3.1 HA/PROT nanoparticles: Formation and formulation variables

Higher concentrations of PROT and lower HA/PROT mass mixing ratios (MMRs) generally resulted in the formation of more turbid systems (Fig. 1A). Samples produced using a solution with a higher HA concentration (1.43 mg/ml) were generally less transparent than those produced using a solution with lower HA concentration (0.71 mg/ml). Phase separation (detected visually as particle flocculation) was observed for an HA/PROT MMR of 1.4 (0.42 PROT weight fraction, PROT concentration of 0.51 mg/ml) and 1.6 (0.39 PROT weight fraction, PROT concentration of 0.91 mg/ml) when HA solutions with concentrations of 0.71 and 1.43 mg/ml, respectively, were used.

The effect of the molecular weight of HA on the transmittance of the formulations was also investigated. Transmittance values of the 0.71-mg/ml HA-based NPs did not differ significantly when HA with different molecular weights of 590 kDa, 257 kDa and 176 kDa were used (Fig. 1A). However, when native HA (as supplied) with a molecular weight of 2882±24.50 kDa was used, the formation of microparticles and/or quick-sedimenting NP aggregates was observed when lower PROT concentrations (e.g., 0.06 mg/ml or 0.11 mg/ml, equivalent to an HA/PROT MMR of 12.5 and 6.3 of PROT, respectively) were used. As

previously presented by Umerska et al., NP aggregates developed when HA reacted with another polycation or chitosan due to the high molecular weight HA (1161 kDa and above) and high viscosity of its solution.[4] The hydrodynamic diameter of the HA/PROT NPs increased gradually with the increasing amount of added protamine (Fig. 1B). Neither the molecular weight (between 590 kDa and 176 kDa) nor the concentration of HA (0.71 mg/ml or 1.43 mg/ml) appeared to have a significant effect on the size of the particles formed. It is noteworthy that the HA/PROT NPs appear as rather small polyelectrolyte-complex NPs with sizes well below 100 nm in certain systems. To the best of our knowledge, the complexation of HA to PROT described in this work resulted in the formation of one of the smallest HA-based polyelectrolyte complex NPs (58±18 nm for an HA/PROT MMR of 12.5; HA257). Kim et al. succeeded in producing HA-containing (HA with a molecular weight of 19 kDa) NPs smaller than 100 nm (89±12 nm) via complexation to polyarginine.[8] Mayer et al. highlighted that substitution of protamine-free base by protamine sulfate greatly reduced the size of oligonucleotide-protamine-albumin nanoparticles from 200 nm to approximately 40 nm (43 and 48 nm by sedimentation velocity analysis and 40 nm by atomic force microscopy).[22] Additionally, Mok et al. showed that the particle size of the NPs was reduced from 654 nm to 166 nm when HA was first conjugated to oligodeoxynucleotides and subsequently complexed with protamine compared with the NPs from a system formed by complexing naked oligodeoxynucleotides with HA and protamine[15]. Other HA-complex NPs with polyarginine[9] and chitosan[1,4] reported to date were significantly larger than 100 nm in diameter.

The transmittance, which gives information on the turbidity of the sample, depends on the concentration and the particle size of the nanocomplexes. An increase in the particle size (Fig. 1B) was accompanied by a decrease in transmittance (i.e., the samples became more turbid). In addition, samples with higher concentration of HA and PROT (HA of 1.4 mg/ml)

were significantly more turbid compared with samples with lower concentrations of polyelectrolytes (HA of 0.71 mg/ml). Because there was no statistically significant difference in the particle size of these samples, the decreased transmittance may be attributed to the increase in the concentration of NPs.

The investigated NP formulations had low PDI values generally below 0.35 with certain values as low as 0.1, indicating homogenous dispersions (Fig. 1C). The molecular weight of HA had a significant influence on the size distribution, with the 590-kDa HA-based formulations showing the highest PDI values, which decreased gradually from 0.348 to 0.129 with an increasing amount of added PROT. The 257-kDa and 176-kDa HA-based formulations displayed generally lower PDI values (Fig. 1C). The PDI values for the 0.71-mg/ml HA-based NPs at first decreased rapidly with an increasing concentration of PROT and subsequently remained constant or fluctuated slightly for HA/PROT MMR levels of 2.5 and lower. The PDI values of the 1.43-mg/ml HA-based formulations at first decreased slightly, reached a minimum at an HA/PROT MMR of 3.1 and subsequently increased.

Stable (non-sedimenting and non-aggregating) NPs were characterized by negative zeta potential values. The surface charge of the particles was observed to increase with the increasing amount of added PROT (Fig. 1D), consistent with the increasing proportion of the polycation in the NPs. Additionally, the molecular weight of HA and its concentration considerably impacted the zeta potential values of the particles. Despite the changes in zeta potential values, all formulations showed similar pH values ranging between 5.57 and 6.25, and the pH decreased slightly with the increasing amount of PROT in the formulations.

The formulations presented in Fig. 1 showed negative surface potentials, and thus attempts were carried out to obtain positively charged particles because they could be promising carriers for encapsulation/adsorption of negatively charged macromolecules. Experiments showed that after mixing 1 mg/ml of PROT and 1 mg/ml of 176-kDa HA

solutions at an HA/PROT MMR of 0.2, it was possible to obtain small and homogenously dispersed nanoparticles (with initial values for PS and PDI of 252±2.3 nm and 0.065±0.003, respectively); however, their surface charge was notably low (5.5-7 mV), and sedimentation occurred after a few hours of storage at room temperature. Fig. 2 shows the kinetics of aggregation of these particles; the particle size increased rapidly at first within ~2 hours and subsequently reached a plateau for up to 20 hours of storage (Fig. 2). After 22 hours of storage, the presence of micron-size aggregates was evident from the DLS measurements. However, the PDI value increased rapidly from 0.065±0.003 to 0.187±0.006 after 30 minutes, and small variations in the DPI values were observed for the next ~2.5 hours, followed by a dramatic increase to 0.592±0.099 after another 17 hours of storage, accompanied by visible aggregation of the particles (Fig. 2). The values of the zeta potential fluctuated between ~7.3 mV and 5.5 mV and did not change significantly after 22 hours.

In contrast with the results presented above, physically stable and positively charged NPs were formed when HA and polyarginine[8,9] were used together with HA and chitosan[4]. A possible explanation might be the largely different molecular weights of the components used because the molecular weight of HA used in the positively charged NPs was ~35 times higher than the molecular weight of the major component of protamine (5.1 kDa based on manufacturer's data). According to Boddohi et al., when the polyelectrolyte in excess (protamine in this case) has a much lower molecular weight than the other polymer (HA), a more compact morphology results, leading to flocculation of the NPs in certain cases and poor colloidal stability.[23] However, the difference in charge density together with the difference in molecular weight also may be an important factor that causes the poor stability of positively charged HA/PROT NPs. Schatz et al. examined polyelectrolyte complexes composed of chitosan and dextran sulphate.[24] When these researchers mixed a high-Mw chitosan (365 kDa) and a low-Mw dextran sulfate (5 kDa), the situation was similar to that

described above: the polyelectrolyte pair was composed of long molecules with a low charge density and small molecules with a high charge density. When chitosan was used in excess, stable and positively charged particles were obtained; however, when dextran sulfate was used in excess, the negatively charged polyelectrolyte complexes showed poor colloidal stability. Nonetheless, the positively charged polyelectrolyte complexes between HA and polyarginine obtained by Oyarzun-Ampuyero et al. were reported as stable despite the large differences in charge density and chain length of both molecules.[9] The ratio of the molecular weight of the components used by Schatz et al.[24] was 73, that used by Oyarzun-Ampuyero et al.[9] was 11-33, and that of the HA/PROT NPs in the current work was 35.

Another difference between the HA/PROT complex and other polyelectrolyte complexes (e.g., HA/chitosan[3,4], heparin/chitosan[3] and chitosan/dextran[24]) is the decrease in the hydrodynamic diameter of the latter complexes during titration with the oppositely charged polyelectrolyte until a secondary aggregation was obtained preceding irreversible flocculation. Boddohi et al. deduced that this behavior indicates that the particles are composed of a relatively dense hydrophobic core and a less defined hydrophilic corona, with the corona undergoing contraction upon the addition of the oppositely charged polyelectrolyte.[3] However, the size of HA/PROT particles gradually increased at higher PROT concentrations, indicating a different mechanism of complex formation and thus a different structure of HA/PROT NPs. A similar behavior (i.e., an increase in the particle size corresponding to an increasing content of PROT in the formulation and increasing PROT/oligonucleotide MMR) was observed by Junghans et al. for PROT/oligonucleotide NPs.[12]

3.2 Morphology of HA/PROT NPs

Transmission electron micrographs show that the HA/PROT NPs (Fig. 3) were approximately spherical in shape. In certain cases, deformations were observed. However, in

contrast with the HA/chitosan chloride NPs[4], no core and corona structure was observed in the HA/PROT NPs. The particles composed of HA (0.71 mg/ml) and PROT (0.11 mg/ml, HA/PROT MMR=6.3) had sizes of approximately 20 nm to 30 nm (Fig. 3A). Differences in the particle size between the DLS and TEM data are due to the different principles of measurement for both methods and possible modification of a subset of the properties of the particles during sample preparation for TEM, primarily as a result of water removal, as observed previously.[25] In the sample containing additional PROT (0.34 mg/ml) and therefore a smaller ratio of HA to the polycation, the particles observed in the TE micrographs were approximately 100-200 nm in size (Fig. 3B).

Fig. 4 shows SEM micrographs of the HA/PROT NPs. The SEM images confirm the presence of well-developed nanostructures, spherical or spheroidal in shape, that form irregular assemblies depending on the HA concentration and HA/PROT MMR.

3.3 Isoelectric point of HA/PROT nanoparticles

The IEP values of selected HA/PROT NPs are shown in Table 1. Because the NPs are composed of polyelectrolytes sensitive to pH changes, the IEP displays the pH at which particle aggregation/flocculation may occur due to the charge neutralization. Formulations with an HA/PROT MMR of 6.3 did not present an isoelectric point at pH values above 2, and therefore, it is likely that their negative charge would be maintained upon exposure to an environment with low pH. When the concentration of PROT used to form the NPs was increased and thus the HA/PROT MMR was decreased to 3.1, the charge of the particles became neutralized at pH ranges of 2.61±0.63 and 1.95±0.34. A further decrease in the HA/PROT MMR to 2.1 resulted in an increase in the IEP value to 2.90±0.05. Therefore, it can be concluded that the IEP of the HA/PROT NPs depends primarily on the HA/PROT MMR. However, the IEP values with an HA/PROT MMR of 3.1 based on HA with different molecular weights did not differ significantly, and therefore, the molecular weight of HA used

does not seem to affect the pH at which the charge of the NPs is neutralized. A similar trend, (i.e., dependence of IEP on the polyanion/polycation mixing ratio) was observed in previously described HA/chitosan NPs.[4] The IEP values of HA/PROT NPs were comparable with those of HA/chitosan NPs with similar MMRs.[4]

3.4 Stability studies of HA/PROT NPs upon storage at room temperature

Three formulations based on 0.71-mg/ml HA257 were selected for stability studies at room temperature (formulations FA, FB and FC with MMRs of 6.3, 3.1 and 2.1, respectively). Early signs of sedimentation were observed for all three formulations after two weeks of storage. The changes in the properties of the systems are shown in Fig. 5.

The transmittance of FC, which was the most turbid of all the formulations tested, did not change significantly during four weeks of storage, and the transmittance of other formulations (FA and FB) systematically decreased over the first two weeks of storage (Fig. 5A). After four weeks of storage, however, the FA became more transparent, and a significant increase was observed in the transmittance values between weeks 3 and 4, which may be attributed to sedimentation of aggregating particles.

The particle sizes of FA and FB increased gradually and significantly for the first three weeks of storage, whereas the size of the particles in formulation FC remained unchanged (Fig. 5B). The increase in the particle size occurred earlier for FA compared FB; however, even after three weeks of storage, the FA particles were still significantly smaller than those of FB. After four weeks of storage, a significant increase in the particle size was observed for all formulations tested and was especially pronounced in FA. The PDI of FA and FB decreased noticeably in the first days of storage, whereas the PDI of FC generally remained steady up to three weeks of storage. However, after the fourth week of storage, a significant decrease in the homogeneity of the NPs of all three formulations was observed, which corresponds to the increase in the particle size (Fig. 5C).

The surface charge of the particles became less negative during storage, and the increase was most pronounced in formulation FA (Fig. 5D). After two weeks of storage, the zeta potential values of FA, FB and FC were all significantly different from one another, but there was no statistically significant difference between FA and FB after three weeks. After four weeks, there was no significant difference between all three formulations.

Although the NPs appeared to be relatively stable after one or even two weeks of storage, it can be observed that the systems are dynamic. It is likely that the particles interacted, leading to changes and re-organization in their structures. The PROT NPs were found to be less stable than the previously described HA/chitosan NPs.[4] This difference is especially pronounced for positively charged NPs (see Section 3.1) and may be due to the fact that the charge density of the polycations is different and that the molecular weight of chitosan is over 20-fold greater than that of PROT. Interestingly, the PROT/oligonucleotide nanoparticles described by Junghans et al. with mean diameters of 150-170 nm doubled their size after three days, reaching diameters of approximately 300 nm.[12] The formulation tested by Junghans et al. had a positive surface charge, and no data on the stability of negatively charged PROT/oligonucleotide NPs were provided.

3.5 Formation and characterization of sCT-loaded HA/PROT NPs

Table 2 shows the composition of the sCT-loaded HA257/PROT nanoformulations tested. The formulations containing different concentrations of HA and PROT were selected to examine the influence of HA and PROT concentration and their mixing ratios on the properties of the sCT-containing NPs. In addition, different concentrations of sCT were used to examine the effect of this variable on the formation and properties of the NPs. Dispersions with an HA/PROT MMR=1.8 (containing the greatest proportion of PROT) were not considered as viable delivery systems because they were not physically stable due to their low surface charge. The properties of the sCT-loaded NPs investigated are presented in Table 2.

Similar to the HA/PROT NPs without sCT, the higher the concentration of PROT, the lower the transmittance measured (Table 2). Low concentrations of sCT (0.1 mg/ml) did not have a significant influence on the turbidity of the dispersions, but when the concentration of sCT was increased to 0.5 mg/ml or 1 mg/ml, it was evident that the formulations became less transparent. Additionally, the increase in the HA concentration led to the formation of more turbid HA/PROT/sCT systems, and the formulations based on 1.43-mg/ml HA solutions were characterized by lower transmittance values compared with those of the equivalent 0.71-mg/ml HA-based formulations (Table 2).

The presence of sCT in the particles had a considerable impact on their properties. An increase in the amount of sCT markedly increased the size of the particles (Table 2). It could be possible that the repulsion between the positive charges of PROT and sCT (sCT has an IEP of 10.2[26]) are responsible for the increase in the size of the sCT-loaded NPs. The measured decrease in the transmittance values may be also attributed to the increasing size of the particles. A sample SEM of NPs containing sCT is shown in Fig. 4F. As shown in the micrographs, the morphologies of the peptide-loaded NPs did not vary substantially from that of the equivalent empty particles.

Most of the sCT-loaded formulations investigated had PDI values smaller than 0.25, (Table 2), but no clear relationship between the amount of sCT present and PDI values was discerned. Only the least stable formulations (HA/PROT MMR=2.1) had significantly increased PDI values. This increase was accompanied by an increase in the particle size and was observed after a few hours precipitation.

Incorporation of sCT into the NPs decreased the surface charge of the particles in a concentration-dependent manner; however, all formulations remained negatively charged (Table 2). This observation may indicate that an amount of sCT was deposited on the surface of the particles. Nevertheless, many formulations (especially those with low sCT content)

were still characterized by a highly negative surface charge, even after incorporation of the peptide into the NPs. In certain cases, loading of sCT led to an increase in the zeta potential to values close to -20 mV, and this rise was especially pronounced in formulations containing higher amounts of PROT. Table 1 shows that a loading of 0.5 mg/ml of sCT did not affect the isoelectric point of the 0.71-mg/ml HA-based formulation with an HA/PROT MMR of 6.3. Therefore, sCT could be safely loaded into the NPs that contained a low amount of PROT without significantly changing their behavior in acidic environments.

As shown in Table 2, sCT was successfully associated with the HA/PROT nanoparticles. The association efficiency (AE) values were quite high (most were greater than 90%) and can be considered as one of the highest value reported thus far for sCT. Certain authors managed to obtain AE values higher than 90% (e.g., Yang et al.[27]), but many authors reported much lower values (e.g., Makhlof et al. - 64%[28] and Cetin et al. - 69%[29]). Only the formulations with higher amounts of PROT relative to HA (i.e., F6 and F11) were characterized by slightly lower AEs. Formulations with greater HA content and greater HA/PROT MMRs were capable of associating additional sCT (e.g., F7, in which more than 98% of sCT was effectively associated with the particles despite the fact that the concentration of sCT of 1 mg/ml was the highest that was tested).

Another important parameter complementary to AE is the drug loading, which is defined as the mass of sCT to the total mass of NPs. High drug loading values are desired for achieving therapeutic concentrations and minimizing possible toxic effects of the carrier. The HA/PROT NPs had rather high sCT loading values, approaching 52% w/w. This characteristic is undoubtedly one of the key advantages of HA/PROT NPs over other sCT-containing NPs, such as PLGA-based NPs, in which it is necessary to use high polymer concentrations to successfully bind the active ingredient. For instance, Glowka et al. achieved only a 0.2% w/w loading of sCT in PLGA NPs despite high encapsulation efficiency values

(up to 83%).[30] High loading capacities for polyelectrolyte complex NPs have previously been reported for other compounds, e.g., Oyarzun-Ampuyero et al. loaded ~60% w/w of heparin into chitosan-based NPs.[31]

It was evident that formulations with higher concentration of PROT or lower HA/PROT MMR were capable of loading smaller amounts of sCT. Additionally, higher sCT concentrations caused aggregation of the particles. For example, F6 and F11 were characterized by the least favorable properties (i.e., highest particle size and PDI, a relatively high surface charge and the lowest AE values of all formulations tested).

Because the IEP of sCT is 10.2, it is therefore expected that the peptide will bear a positive charge under all formulation conditions tested. The PROT, which is an arginine-rich protein with an IEP of ~12, bears a stronger positive charge than sCT. Therefore, after incorporation of PROT into the HA/sCT dispersion, competition is likely between these two positively charged macromolecules for binding with negatively charged carboxylic groups of HA. The interaction of PROT with HA should be much stronger than that of sCT according to Coulomb's law, and thus, it is not recommended to have an excess of PROT in the formulation because it limits the amount of sCT that might be loaded into the particles (e.g., F6 and F11). The presence of PROT is necessary for the NPs to develop because no colloidal-size particulates were formed when sCT was dissolved in HA solutions. It also can be hypothesized that sCT (as a polycation under the conditions tested) can interact with HA (the polyanion) via electrostatic interactions. Indeed, the formation of protein/polysaccharide complexes is dominated by electrostatic interaction.[32] Van Damme et al., who examined the interactions between HA and lysozyme (which has an IEP similar to sCT) confirmed the electrostatic nature of such interactions.[6] Thus, when an excess of PROT is added into the formulation, sCT may be released from its complex with HA and be deposited on the negatively charged surface of the particles, resulting in a decrease in the surface charge and

aggregation of particles. This process may have occurred in formulations F6, F10 and F11, which were deemed unstable and in which precipitation was observed after a few hours of storage. These formulations were also susceptible to precipitation during separation of non-associated sCT via ultrafiltration-centrifugation.

In conclusion, because sCT has a destabilizing effect on the NPs, especially when used at high concentrations (e.g., 1 mg/ml), it is necessary to compensate for this effect using low PROT concentrations.

3.6 sCT release studies from HA/PROT nanoparticles

The results of *in vitro* release studies are shown in Fig. 6. The release profiles of sCT may be considered similar for all formulations tested. Although the percentage of sCT released from F6 was slightly lower, even in this case, the difference was not statistically significant. Formulation F6 was one of the most unstable formulations (the particles aggregated quickly in PBS to form entities with sizes of 623±87 nm), and it is possible that sCT was irreversibly bound to the aggregated fraction. No aggregation or flocculation was observed for other samples tested in the release medium (PBS), and the particle size of the systems decreased in general, suggesting a degree of NP dissolution. For instance, the F3 particle size decreased from 211±28 nm to 159±6 nm and that of F11 was reduced from 505±133 nm to 244±24 nm.

Approximately half of the sCT dose loaded into the NPs was released in the first 2 hours, and up to approximately 70-80% of sCT was released after 24 hours (Fig. 6). The release of sCT from the HA/PROT NPs is relatively rapid compared with other delivery systems that are capable of providing release of proteins for days.[33] The rate of protein release from ionic hydrogels is influenced by the various structural parameters of the protein and polyelectrolyte as well as the environmental conditions inside hydrogel.[34] Proteins with low molecular weights are generally characterized by faster release rates.[34] Additionally, Kamiya

and Klibanov examined the release of lysozyme from its complexes with different polyanions.[35] These researchers confirmed that the protein was gradually released from its non-covalent and water-insoluble complex with the oppositely charged poly-ion over a period of hours or days, and the rate of *in vitro* release was markedly dependent on the nature of the polyion. Polymers with higher charge density were found to provide slower release of lysozyme. Because HA has rather low charge density and sCT is a peptide with low molecular weight, it is expected that most of the sCT release would occur within a few hours.

The release data were fitted to a first-order equation (Eqn. 3, Section 2.4), and the parameter estimates obtained are summarized in Table 3. For the 1-mg/ml sCT, sample F3 (HA/PROT MMR of 6.3, HA concentration of 0.7 mg/ml) had the largest W_∞, and statistically significantly lower W_∞ values were obtained for NPs with an HA/PROT MMRs of 4.2 (F8) and 3.1 (F9) (HA concentration of 1.4 mg/ml). These results are therefore in agreement with the above observation that superior sCT carriers consist of those with low PROT content. When 0.5-mg/ml sCT was used, the W_∞ were observed to be significantly different for samples based on 0.71-mg/ml HA with an MMR of 6.3 (F2) and 2.1 (F6). Comparison of the release data from samples with the same MMR (3.1) and different HA concentrations revealed that the W_∞ values were statistically significant and greater for NPs composed of 0.7-mg/ml HA than those prepared from 1.4-mg/ml HA. Therefore, it appears that the additional HA present in NPs is able to bind more sCT, and thus the total amount of sCT released is lower. Greater amounts of PROT result in greater W_∞ values, consistent with the hypothesis of species competition (PROT versus sCT) in binding with HA.

Analysis of the release data led to the conclusion that the driving force for release of sCT was initially dissolution of the NPs (break-up of complexes due to the higher ionic strength of PBS) and diffusion of the peptide across the NP matrix due to the concentration gradient. However, as indicated by the W_∞ values (Table 3), a certain amount of sCT

remained strongly complexed to HA and was not released under the conditions of the experiment.

3.7 Effect of formulation on enzymatic degradation of sCT

As shown in Fig. 7, the sCT was not degraded in all control samples if no enzyme were present. The amount of intact peptide was not statistically different if comparing the quantity of peptide recovered from the sCT solutions and NP formulations at the different time points. In the presence of pepsin, the stability of sCT in the NPs was significantly improved up to 60 min of incubation (Fig. 7A) in contrast with the results obtained for the sCT solution. The NPs appeared to protect the peptide associated with the NPs for up to 30 min in the trypsin environment, but the sCT was degraded in all samples (the amount of peptide recovered from the NP system was 3.7±1.5% vs. a solution of 0.8±0.1% after 30 minutes of the experiment) when exposed to the enzyme for 30 min or longer (Fig. 7B). Therefore, it can be concluded that the formulation can protect the peptide *in vitro* from enzymatic degradation by pepsin and trypsin. Lee et al. reported on the preparation and characterization of an sCT–sodium triphosphate ionic complex for oral delivery of the peptide and observed that the complex protected the sCT from enzymatic cleavage by pancreatin[36]. Thus, it appears that polyelectrolyte complexes can be robust and have protective effects on the associated peptide.

The PROT has been reported to translocate itself into several mammalian cell lines quite efficiently in 30 minutes.[37] In addition, studies showed that PROT was able to carry a peptide gelonin (a plant toxin of approximately 30 kDa) across the membrane after 30 min of incubation of the peptide with CT-26 cells.[37] Furthermore, because HA exhibits mucoadhesive properties in the intestinal environment[38], it can be expected that an intimate contact would be formed[39] between the intestinal mucosa and the nanoparticle, therefore further avoiding degradation of sCT on the path between the carrier and the membrane. Thus

it is expected that even though short in duration, the protective effects of NPs may translate into a real therapeutic effect.

3.8 Cytotoxicity studies

The cytotoxicity of the PROT and NPs was examined in Caco-2 cells to assess any potential toxic interactions with cells. As mentioned previously, HA was not toxic to Caco-2 cells even at a concentration of 5 mg/ml.[4]

An MTS assay and flow cytometry showed that PROT exerts concentration-dependent toxic effects in Caco-2 cells (Fig. 8A). The MTS assay was more sensitive than flow cytometry (IC_{50} of 0.24±0.01 and 0.52±0.03 mg/ml, respectively). It can be observed from apoptosis assay results (Fig. 8B) and the scatter plots (Fig. 8C) that higher concentrations of PROT considerably increased the number of cells in late apoptosis or the number of dead cells. Additionally, exposure to higher concentrations of PROT (0.5 mg/ml and higher) significantly ($p=0.020$) increased the number of early apoptotic cells compared with that of the control (7.00±3.11% and 1.83±1.03% of early apoptotic cells, respectively). Mok et al. examined the cytotoxicity of PROT in HEK 293 cells via the CCK-8 cell viability assay, which also depends on the activity of mitochondrial dehydrogenase of the cells, similar to MTS.[15] The maximum concentration of PROT tested (160 µg/ml) did not affect the viability of the cells after 24 hours of incubation. We observed a significant decrease in the viability of cells determined via MTS assay at a PROT concentration of 125 µg/ml (Fig. 8A and 9). The difference may be explained by the markedly longer incubation time (72 hours) used in the current studies and by the use of a different cell line.

The NPs selected for cytotoxicity studies by MTS assay had an HA/PROT MMR of 3.1. This dispersion was stable even after dilutions with medium containing a concentration of PROT sufficiently high to produce a toxic effect on the Caco-2 cells such that a comparison could be carried out on the effects of PROT and HA/PROT NPs. At the highest concentration

of NPs possible to achieve for this formulation, i.e., 0.78 mg/ml of NPs (which contains 0.25 mg/ml of PROT), the viability of the cells was decreased significantly (70.31±15.65% of viable cells) compared with that of serum-free medium (Fig. 9).

The cell viability was comparable after treatment with 0.25 mg/ml of PROT and NPs containing 0.25 mg/ml PROT (Fig. 9). Further 1:1 dilutions of the NPs (with serum-free medium) did not show toxic effects even at 0.39 mg/ml of NPs (containing 0.125 mg/ml of PROT), in contrast to PROT on its own, which at 0.125 mg/ml decreased the amount of living cells by ~20% compared with serum-free medium. The toxic effects seem to be produced primarily by the free polycation (PROT) rather than by the PROT bound to the polyanion (HA) in the NPs. Consequently, the decrease in cell viability observed at the highest NP concentration tested (containing 0.25 mg/ml of PROT) may possibly be caused by the presence of free PROT non-associated with the particles. The increase in pH (from 6 to 7.4) and ionic strength after dispersion of HA/PROT NPs in serum-free medium could weaken the electrostatic interactions between HA and PROT and lead to dissociation of a subset of the HA/PROT nanocomplexes, resulting in release of PROT molecules.

Therefore, it can be suggested that HA present in the NPs exerts a protective effect on Caco-2 cells against the negative influence of PROT, as previously observed for HA/chitosan NPs.[4] The protective effects of HA against the toxicity of another polycation, i.e., polyarginine, have been demonstrated by Kim et al.[8] This group showed that HA/polyarginine nanoparticles were markedly less toxic compared with polyarginine on its own and that increasing the HA content in the formulation further reduced their toxicity.

4. Summary and conclusions

In this work, a new type of nanoparticle carrier was successfully developed that incorporates HA and PROT into its structure. The formation and characteristics of the particles depend on the conditions used, e.g., the concentration of both polyelectrolytes and

their MMR, and also on the molecular weight of HA used. Positively charged nanoparticles were not stable upon storage at room temperature in contrast with dispersions containing negatively charged particles. By modulation of the formulation conditions, it was possible to produce NPs with good micromeritic properties, i.e., monodispersed and with a notably small size. A subset of the nano-suspensions was characterized by a particle size below 100 nm, which can be considered quite small for polymeric nanoparticles. Indeed, the smallest particles containing HA590 and PROT at an HA/PROT MMR of 13 were characterized by an average hydrodynamic diameter of 58±18 nm.

Additionally, most of HA/PROT dispersions tested had an isoelectric point close to a pH of 2, and therefore, it appears that these particles will be stable and will maintain their negative surface charge at neutral and slightly acidic pH values. The HA/PROT NPs showed low toxicity to Caco-2 cells.

The HA/PROT NPs appear to be a promising system for the delivery of sCT because they are characterized by an excellent capacity for loading high doses of sCT and providing prolonged release and protection from enzymatic degradation of this peptide. By optimizing the composition of the nanoparticles, it was possible to obtain sCT-loaded NPs that maintained good physical properties. These HA/PROT NPs also may be considered as a promising system for the delivery of compounds other than sCT.

Acknowledgments

This study was funded by the Irish Drug Delivery Research Network and a Strategic Research Cluster grant (07/SRC/B1154) under the National Development Plan co-funded by EU Structural Funds and Science Foundation Ireland. Author CM is SFI Stokes lecturer, and author KJP is funded by the Solid State Pharmaceutical Cluster, supported by Science Foundation Ireland under grant number 07/SRC/B1158. Author MJSM is an Usher lecturer in

Nanopharmaceutical Drug Discovery, Trinity College Dublin. We acknowledge support from Ireland's Higher Education Authority Programme for Research in Third Level Institutes (HEA PRTLI) Cycle 5 of Trinity Biomedical Sciences Institute.

References:

1. M. de la Fuente, B. Seijo, M. J Alonso, Novel hyaluronan-based nanocarriers for transmucosal delivery of macromolecules, Macromol. Biosci. 8, 441-450 (**2008**).

2. M. de la Fuente, B. Seijo, M. J Alonso, Design of novel polysaccharidic nanostructures for gene delivery, Nanotechnology. 19, 075105-075114 (**2008**).

3. S. Boddohi, N. Moore, P. Johnson, M. Kipper, Polysaccharide-based polyelectrolyte complex nanoparticles from chitosan, heparin, and hyaluronan, Biomacromolecules. 10, 1402-1409 (**2009**).

4. A. Umerska, K. J. Paluch, I. Inkielewicz-Stepniak, M. J. Santos-Martinez, O. I. Corrigan, C. Medina, L. Tajber, Exploring the assembly process and properties of novel crosslinker-free hyaluronate-based polyelectrolyte complex nanocarriers, Int. J. Pharm. 436, 75-87 (**2012**).

5. S. K. Hahn, A. S. Hoffman, Preparation and characterization of biocompatible polyelectrolyte complex multilayer of hyaluronic acid and poly-L-lysine, Int. J. Biol. Macromol. 37, 227-231 (**2005**).

6. M.-P. I. Van Damme, J. M. Moss, W. H. Murphy, B. N. Preston, Binding properties of glycosaminoglycans to lysozyme- effect of salt and molecular weight, Arch. Biochem. Biophys. 310, 16-24 (**1994**).

7. I. Morfin, E. Buhler, F. Cousin, I. Grillo, F. Boué, Rodlike complexes of a polyelectrolyte (hyaluronan) and a protein (lysozyme) observed by SANS, Biomacromolecules. 12, 859-870 (**2011**).

8. E.-J. Kim, G. Shim, K. Kim, I. C. Kwon, Y.-K. Oh, C.-K. Shim, Hyaluronic acid complexed to biodegradable poly L-agrinine for targeted delivery of siRNAs, J. Gene Med. 11, 791-803 (**2009**).

9. F. A. Oyarzun-Ampuero, F. M. Goycoolea, D. Torres, M. J. Alonso, A new drug nanocarrier consisting of polyarginine and hyaluronic acid, Eur. J. Pharm. Biopharm. 79, 54-57 (**2011**).

10. H. C. Hagedorn, Protamine Insulinate, Proc. R. Soc. Med. 30, 805-814 (**1937**).

11. F. Reynolds, R. Weissleder, L. Josephson, Protamine as an efficient membrane-translocating peptide, Bioconjugate Chem. 16, 1240-1245 (**2005**).

12. M. Junghans, J. Kreuter, A. Zimmer, Antisense delivery using protamine-oligonucleotide particles, Nucleic Acids Res. 28, e45 (**2000**).

13. Y. Mori, S. Nakamura, S. Kishimoto, M. Kawakami, S. Suzuki, T. Matsui, M. Ishihara, Preparation and characterization of low-molecular-weight heparin/protamine nanoparticles (LMW-H/P NPs) as FGF-2 carrier, Int. J. Nanomedicine. 5, 147-155 (**2010**).

14. A. Takagi, N. Yamashita, T. Yoshioka, Y. Takaishi, K. Nakanishi, S. Takemura, A. Maeda, K. Saito, Y. Takakura, M. Hashida, Incorporation into a biodegradable hyaluronic acid matrix enhances in vivo efficacy of recombinant human interleukin 11 (rhIL11), J. Control. Release. 115, 134-139 (**2006**).

15. H. Mok, J. W. Park, T. G. Park, Antisense oligodeoxynucleotide-conjugated hyaluronic acid/protamine nanocomplexes for intracellular gene inhibition, Bioconjugate Chem. 18, 1483-1489 (**2007**).

16. S. M. Ryan, J. McMorrow, A. Umerska, H. B. Patel, K. N. Kornerup, L. Tajber, E. P. Murphy, M. Perretti, O. I. Corrigan, D. J. Brayden, An intra-articular salmon calcitonin-based nanocomplex reduces experimental inflammatory arthritis, J. Control. Release. 167, 120-129 (**2013**).

17. EMEA website, EMA/H/A-31/1291, Questions and answers on the review on calcitonin-containing medicines. http://www.ema.europa.eu/docs/en-GB/document_library/Referrals_document/Calcitonin_31/WC500130149.pdf, Accessed on 10th September 2013

18. K. J. Paluch, L. Tajber, O. I. Corrigan, A. M. Healy, Impact of process variables on the micromeritic and physicochemical properties of spray-dried porous microparticles, part I: introduction of a new morphology classification system, J. Pharm. Pharmacol. 64, 1570-1582 (**2012**).

19. D. O. Corrigan, A. M. Healy, O. I. Corrigan, Preparation and release of salbutamol from chitosan and chitosan co-spray dried compacts and multiparticulates, Eur. J. Pharm. Biopharm. 62, 295-305 (**2006**).

20. European Pharmacopoeia (Ph. Eur.), 7th edition, The European Directorate for the Quality of Medicines & Health Care (**2010**).

21. S. Goutelle, M. Maurin, F. Rougier, X. Barbaut, L. Bourguignon, M. Ducher, P. Maire, The Hill equation : a review of its capabilities in pharmacological modeling, Fundam. Clin. Pharm. 22, 633-648 (**2008**).

22. G. Mayer, V. Vogel, J. Weyermann, D. Lochmann, J. A. van den Broek, C. Tziatzios, W. Haase, D. Wouters, U. Schubert, A. Zimmer, J. Kreuter, D. Schubert, Oligonucleotide-protamine-albumin nanoparticles: protamine sulfate causes drastic size reduction, J. Control. Release. 106, 181-187 (**2005**).

23. S. Boddohi, M. J. Kipper, Engineering nanoassemblies of polysaccharides, Adv. Mater. 22, 2998-3016 (**2010**).

24. C. Schatz, A. Domard, C. Viton, C. Pichnot, T. Delair, Versatile and efficient formation of colloids of biopolymer-based polyelectrolyte complexes, Biomacromolecules. 5, 1882-1892 (**2004**).

25. L. Jr. Lapčík, L. Lapčík, S. De Smedt, J. Demeester, P. Chabreček, Hyaluronan: preparation, structure, properties and applications, Chem. Rev. 98, 2664-2683 (**1998**).

26. T. Tsai, R. C. Mehta, P. P. DeLuca, Adsorption of peptides to poly(d,l-lactide-co-glycolide): 2. Effect of solution properties on the adsorption, Int. J. Pharm. 127, 43-52 (**1996**).

27. M. Yang, H. Yamamoto, H. Kurashima, H. Takeuchi, T. Yokoyama, H. Tsujimoto, Y. Kawashima, Eur. J. Pharm. Sci. 46, 374-380 (**2012**).

28. A. Makhlof, M. Werle, Y. Tozuka, H. Takeuchi, Nanoparticles of glycol chitosan and its thiolated derivative significantly improved the pulmonary delivery of calcitonin, Int. J. Pharm. 397, 92-95 (**2010**).

29. M. Cetin, M. S. Aktas, I. Vural, M. Ozturk, Salmon calcitonin-loaded Eudragit® and Eudragit®-PLGA nanoparticles: in vitro and in vivo evaluation, J. Microencapsul. 29, 156-166 (**2012**).

30. E. Glowka, A. Sapin-Minet, P. Leroy, J. Lulek, P. Maincent, Preparation and *in-vitro- in vivo* evaluation of salmon calcitonin loaded polymeric nanoparticles, J. Microencapsul. 27, 25-36 (**2010**).

31. F. A. Oyarzun-Ampuero, J. Brea, M. I. Loza, D. Torres, M. J. Alonso, Chitosan-hyaluronic acid nanoparticles loaded with heparin for the treatment of asthma, Int. J. Pharm. 381, 122-129 (**2009**).

32. R. A. Ganzevles, H. Kosters, T. Van Vliet, M. A. Cohen Stuart, H. H. J. de Jongh, Polysaccharide charge density regulating protein adsorption to air/water interfaces by protein/polysaccharide complex formation, J. Phys. Chem. B. 111, 12969-12976 (**2007**).

33. O. I. Corrigan, X. Li, Quantifying drug release from PLGA nanoparticulates, Eur. J. Pharm. Sci. 37, 477-485 (**2009**).

34. C. L. Cooper, P. L. Dublin, A. B. Kayitmazer, S. Turksen, Polyelectrolyte-protein complexes, Curr. Opin. Colloid Interface Sci. 10, 52-78 (**2005**).

35. N. Kamiya, A. M. Klibanov, Controling the rate of protein release from polyelectrolyte complexes, Biotechnol. Bioeng. 82, 590-594 (**2002**).

36. H. E. Lee, M. J. Lee, C. R. Park, A. Y. Kim, K. H. Chun, H. J. Hwang, D. H. Oh, S. O. Jeon, J. S. Kang, T. S. Jung, G. J. Choi, S. Lee, Preparation and characterization of salmon calcitonin-sodium triphosphate ionic complex for oral delivery, J. Control. Release. 143, 251-257 (**2010**).

37. Y. J, Park, L. C. Chang, J. F. Liang, C. Moon, C. P. Chung, V. C. Yang, Nontoxic membrane translocation peptide from protamine, low molecular weight protamine (LMWP), for enhanced intracellular protein delivery: in vitro and in vivo study, FASEB J. 19, 1555-1557 (**2005**).

38. G. Sandri, S. Rossi, F. Ferrari, M. C. Bonferoni, N. Zerrouk, C. Caramella, Mucoadhesive and penetration enhancement properties of three grades of hyaluronic acid using porcine buccal and vaginal tissue, Caco-2 cell lines, and rat jejunum, J. Pharm. Pharmacol. 56, 1083-1090 (**2004**).

39. D. Guggi, A. Bernkop-Schnürch, In vitro evaluation of polymeric excipients protecting calcitonin against degradation by intestinal serine proteases, Int. J. Pharm. 252, 187-196 (**2003**).

Umerska et al., Self-assembled hyaluronate/protamine polyelectrolyte nanoplexes: Synthesis, stability, biocompatibility and potential use as peptide carriers, Table 1

Table 1. Isoelectric point (IEP) values of HA/PROT nanoformulations.

HA Mw (kDa)	HA (mg/ml)	HA/PROT MMR	sCT (mg/ml)	IEP
257	0.714	6.3	0	1.83±0.29
257	0.714	6.3	0.5	1.66±0.37
257	0.714	3.1	0	1.95±0.34
257	1.429	6.3	0	1.83±0.25
257	0.714	2.1	0	2.90±0.05
257	1.429	3.1	0	2.61±0.63
176	0.714	3.1	0	2.26±0.28
590	0.714	3.1	0	2.25±0.35

Umerska et al., Self-assembled hyaluronate/protamine polyelectrolyte nanoplexes: Synthesis, stability, biocompatibility and potential use as peptide carriers, Table 2

Table 2. Composition, properties (TR – transmittance, PS – particle size, PDI – polydispersity index, ZP – zeta potential), association efficiency (AE), non-associated sCT (N-AE) and sCT loading (DL) of sCT-loaded HA257/PROT formulations tested.

Sample	Initial HA conc. (mg/ml)	MMR	Initial sCT conc. (mg/ml)	TR (%)	PS (nm)	PDI	ZP (mV)	AE sCT (%)	N-AE sCT (%)	DL (%)
F1	0.71	6.3	0.1	94±1	101±15	0.25±0.06	-59.5±0.6	94.7±0.8	99.8±0.0	10.6±0.0
F2	0.71	6.3	0.5	58±15	140±29	0.20±0.07	-38.7±4.2	91.9±2.8	98.4±0.2	37.3±0.1
F3	0.71	6.3	1.0	39±4	211±28	0.17±0.05	-21.6±3.9	81.1±3.4	89.6±2.8	51.9±1.6
F4	0.71	3.1	0.1	77±1	134±8	0.19±0.04	-42.3±2.1	92.4±0.3	99.7±0.1	9.6±0.0
F5	0.71	3.1	0.5	27±5	188±15	0.15±0.05	-24.3±3.6	80.9±4.5	91.4±3.1	32.6±1.1
F6	0.71	2.1	0.5	12±5	409±202	0.30±0.19	-18.2±2.2	64.1±11.6	85.4±4.6	28.8±1.5
F7	1.43	12.5	1.0	67±0	178±12	0.09±0.01	-52.5±1.9	98.1±0.7	98.8±0.0	39.0±0.0
F8	1.43	4.2	1.0	4±0	282±21	0.24±0.02	-37.6±3.7	88.9±1.8	94.8±2.8	34.7±1.0
F9	1.43	3.1	0.5	3±2	273±25	0.21±0.06	-37.1±1.7	89.8±2.0	95.6±2.0	20.2±0.4
F10	1.43	3.1	1.0	2±0	342±70	0.30±0.10	-25.3±2.9	83.5±3.5	90.6±5.0	32.4±1.8
F11	1.43	2.1	0.5	1±0	505±133	0.50±0.13	-26.9±3.5	75.1±3.5	84.7±8.8	16.7±1.7

Table 3. Model parameter estimates for sCT release data fitted to the first-order model (Eqn. 3, Section 2.4), where W_∞ is the amount of sCT released at infinity and k is the release rate constant. The composition of samples is shown in Table 2.

Sample	k (h^{-1})	W_∞ (µg)	Goodness of fit (R^2)
F2	1.20±0.170	291.4±21.8	0.9955
F3	1.17±0.020	397.9±15.3	0.9987
F5	1.12±0.079	246.6±19.4	0.9983
F6	1.27±0.104	200.9±32.1	0.9977
F8	0.98±0.040	287.5±3.99	0.9992
F9	0.92±0.022	160.1±4.35	0.9359
F10	1.16±0.036	251.9±6.86	0.9994
F11	1.16±0.098	127.8±4.27	0.9988

Umerska et al., Self-assembled hyaluronate/protamine polyelectrolyte nanoplexes: Synthesis, stability, biocompatibility and potential use as peptide carriers, Figure 1

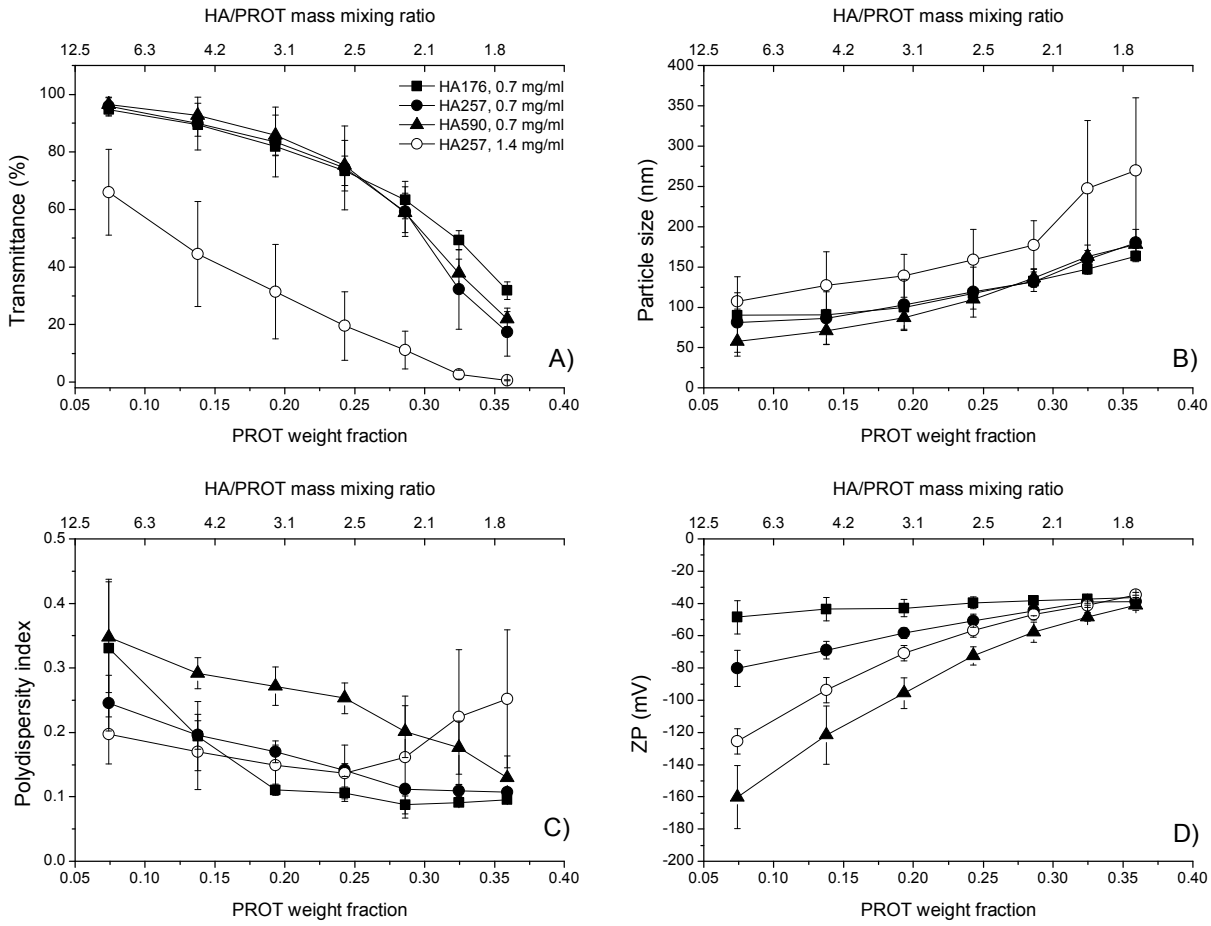

Figure 1. Properties of HA/PROT NPs: A) transmittance, B) particle size (PS), C) polydispersity index (PDI) and D) zeta potential (ZP). Filled squares indicate NPs composed of HA 176 kDa (HA conc. 0.7 mg/ml), filled circles - HA 257 kDa (HA conc. 0.7 mg/ml), filled triangles - HA 590 kDa (HA conc. 0.7 mg/ml) and open circles - HA 257 kDa (HA conc. 1.4 mg/ml) (mean ± S.D., n = 3). Lines are for visual guide only.

Umerska et al., Self-assembled hyaluronate/protamine polyelectrolyte nanoplexes: Synthesis, stability, biocompatibility and potential use as peptide carriers, Figure 2

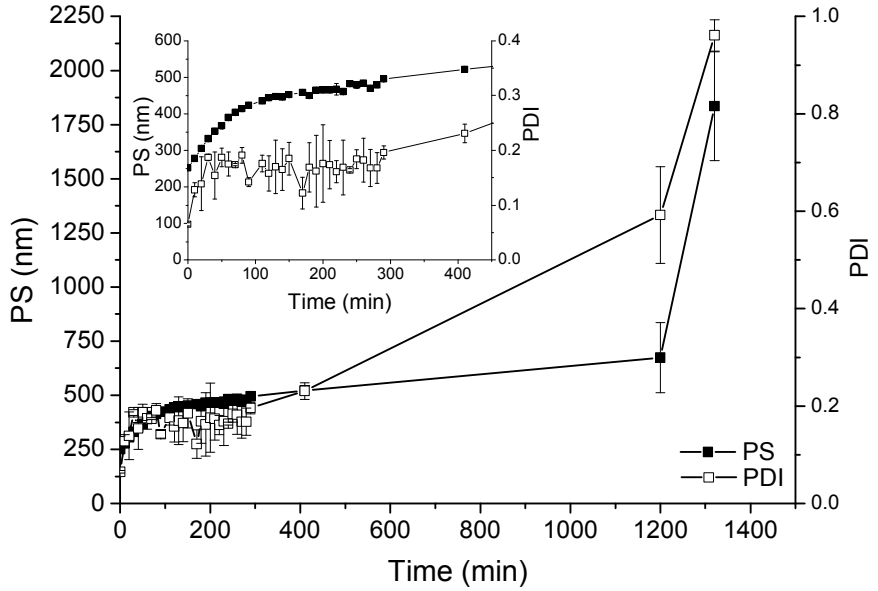

Figure 2. Kinetics of the particle size (PS) and polydispersity index (PDI) changes for positively charged HA257/PROT NPs with an MMR of 0.2 for 22 hours of storage at 25ºC (mean ± S.D., n = 3). Lines are for visual guide only.

Umerska et al., Self-assembled hyaluronate/protamine polyelectrolyte nanoplexes: Synthesis, stability, biocompatibility and potential use as peptide carriers, Figure 3

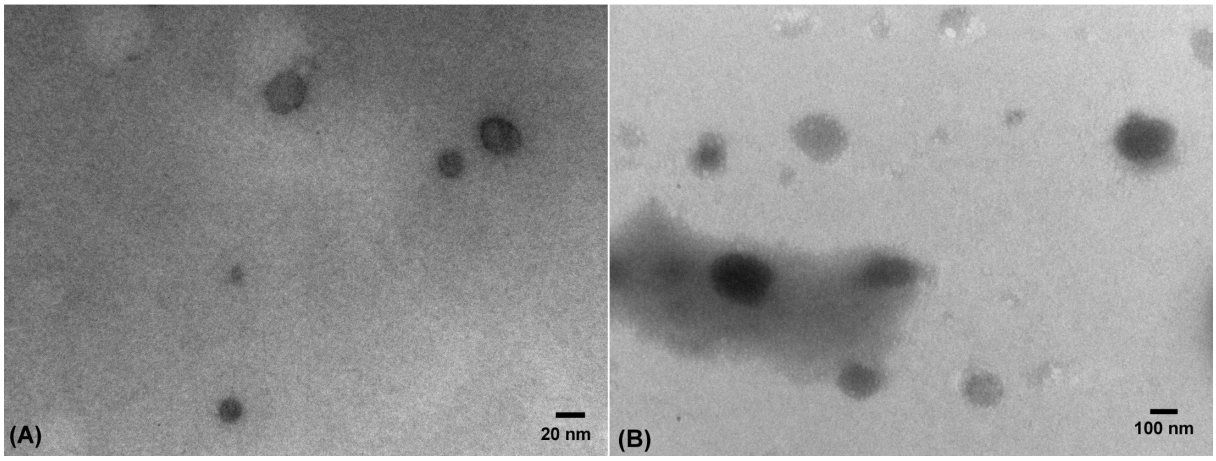

Figure 3. Transmission electron micrographs of HA257/PROT and HA257/PROT/sCT NPs: A) HA=0.7 mg/ml, HA/PROT MMR=6.3 and B) HA=0.7 mg/ml, HA/PROT MMR=2.1.

Umerska et al., Self-assembled hyaluronate/protamine polyelectrolyte nanoplexes: Synthesis, stability, biocompatibility and potential use as peptide carriers, Figure 4

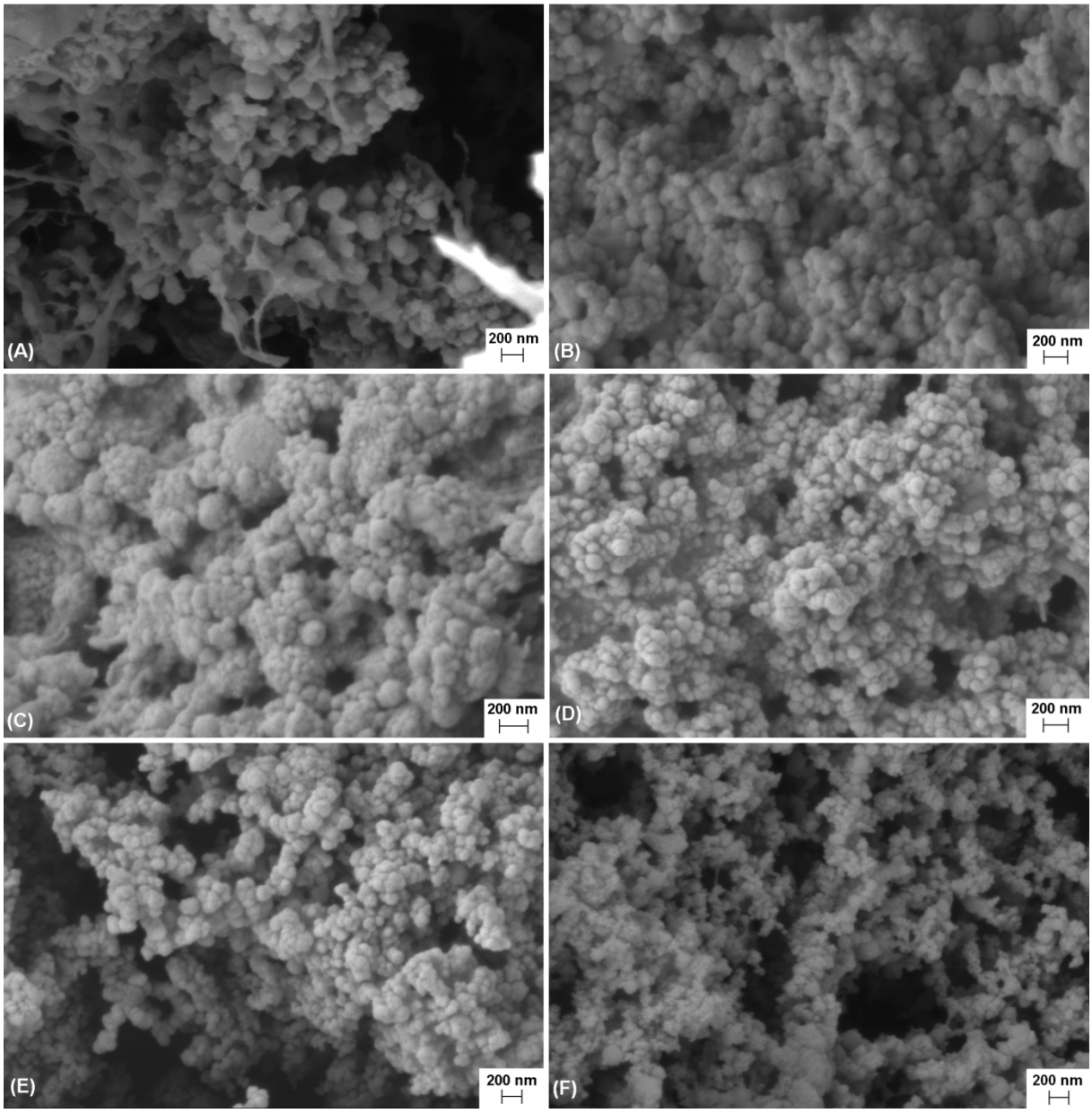

Figure 4. Scanning electron micrographs of HA257/PROT and HA257/PROT/sCT NPs: (A) 0.7 mg/ml HA, HA/PROT MMR=6.3; (B) 0.7 mg/ml HA, HA/PROT MMR=1.8; (C) 1.4 mg/ml HA, HA/PROT MMR=6.3; (D) 1.4 mg/ml HA, HA/PROT MMR=3.1; (E) 0.16 mg/ml HA, HA/PROT MMR=0.2 (positively charged NPs as described in Section 3.1.1) and (F) 0.7 mg/ml HA, HA/PROT MMR=6.3, 0.5 mg/ml sCT.

Umerska et al., Self-assembled hyaluronate/protamine polyelectrolyte nanoplexes: Synthesis, stability, biocompatibility and potential use as peptide carriers, Figure 5

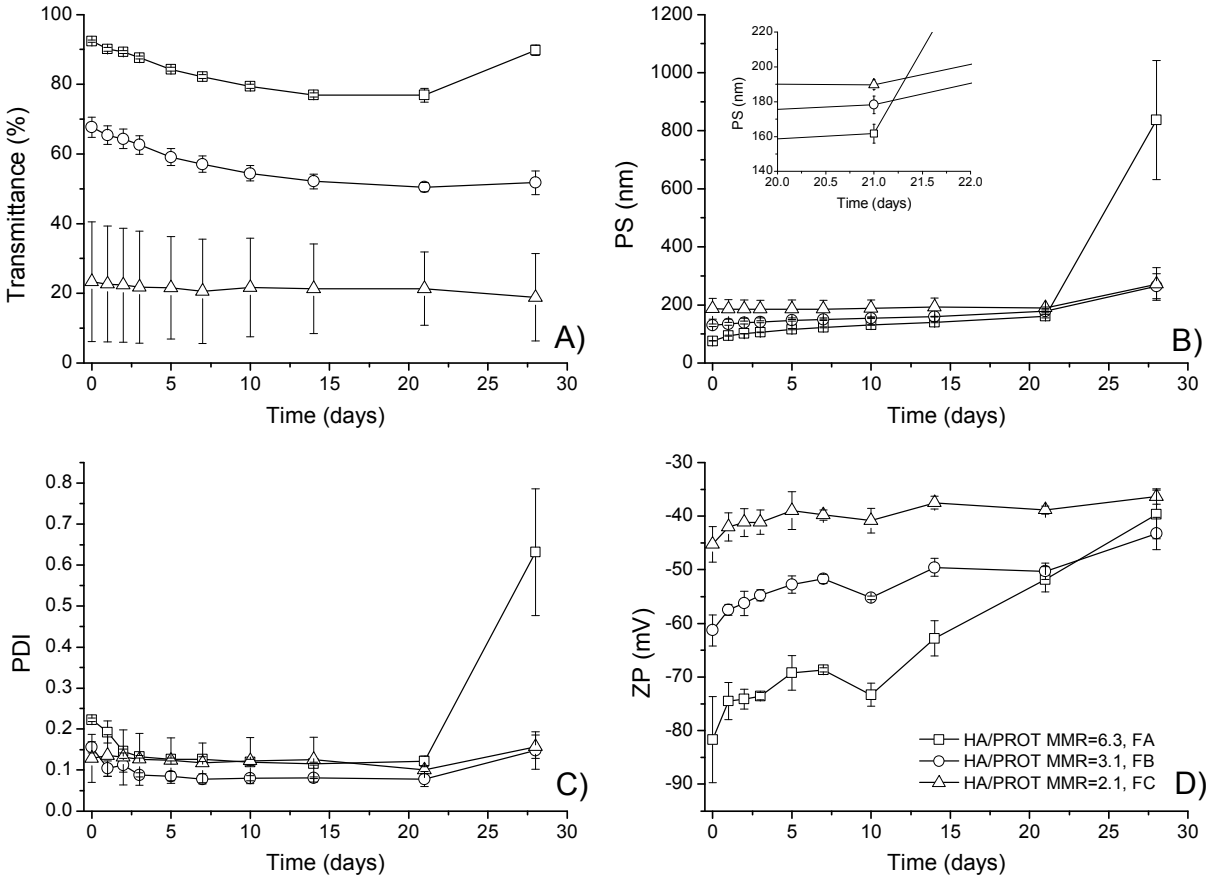

Figure 5. Properties of HA/PROT NPs under storage (stability studies on undiluted dispersions) at room temperature: Transmittance, particle size (PS), polydispersity index (PDI) and zeta potential (ZP). The NPs were composed of 0.71 mg/ml HA257 and had HA/PROT MMRs of 6.3 (sample FA, squares), 3.1 (sample FB, circles) and 2.1 (sample FC, triangles) (mean ± S.D., n = 3). Lines are for visual guide only.

Umerska et al., Self-assembled hyaluronate/protamine polyelectrolyte nanoplexes: Synthesis, stability, biocompatibility and potential use as peptide carriers, Figure 6

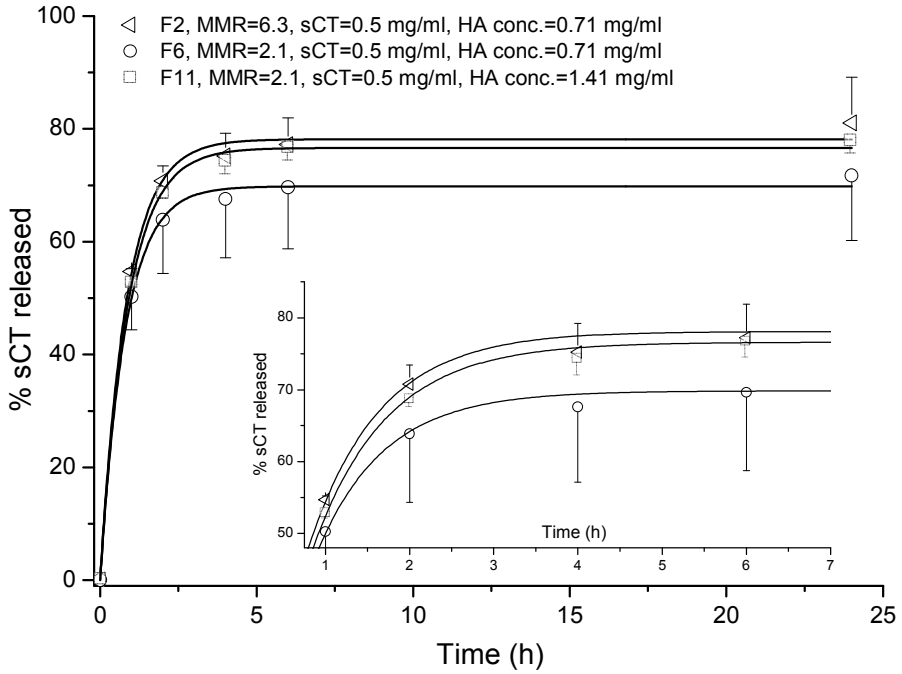

Figure 6. Cumulative release profiles of sCT from different HA257/PROT nanoparticles. The experiments were carried out using PBS (pH 7.4) at 37°C (mean ± S.D., n = 3). Only negative error bars are shown for sample F6, and only positive errors bars are presented for samples F2 and F11 for clarity. The inset shows an enlarged region of the profiles, including data between 1 and 6 hours of the studies. The composition of samples is shown in Table 2. The lines are fitted to the experimental points using a first-order equation (Eqn. 3).

Umerska et al., Self-assembled hyaluronate/protamine polyelectrolyte nanoplexes: Synthesis, stability, biocompatibility and potential use as peptide carriers, Figure 7

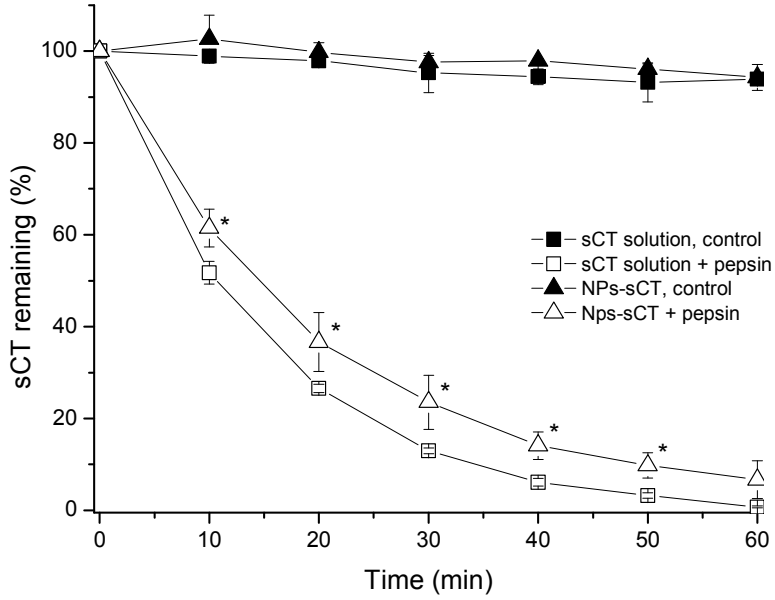

A)

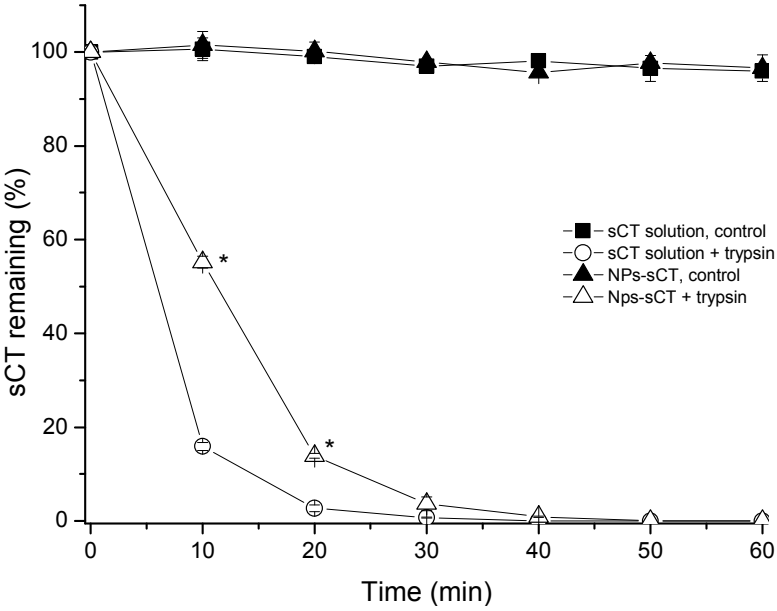

B)

Figure 7. Amount of sCT remaining after incubation of sCT in solution and sCT associated with NPs: A) pepsin in simulated gastric fluid at 37°C (the sCT and pepsin initial concentrations were 0.1 mg/ml and 200 IU/ml, respectively) and B) trypsin in PBS (pH 7.4) at 37 °C (the sCT and trypsin initial concentrations were 0.1 mg/ml and 7 BAEE/ml, respectively) (mean ± S.D., n = 4).

Umerska et al., Self-assembled hyaluronate/protamine polyelectrolyte nanoplexes: Synthesis, stability, biocompatibility and potential use as peptide carriers, Figure 8

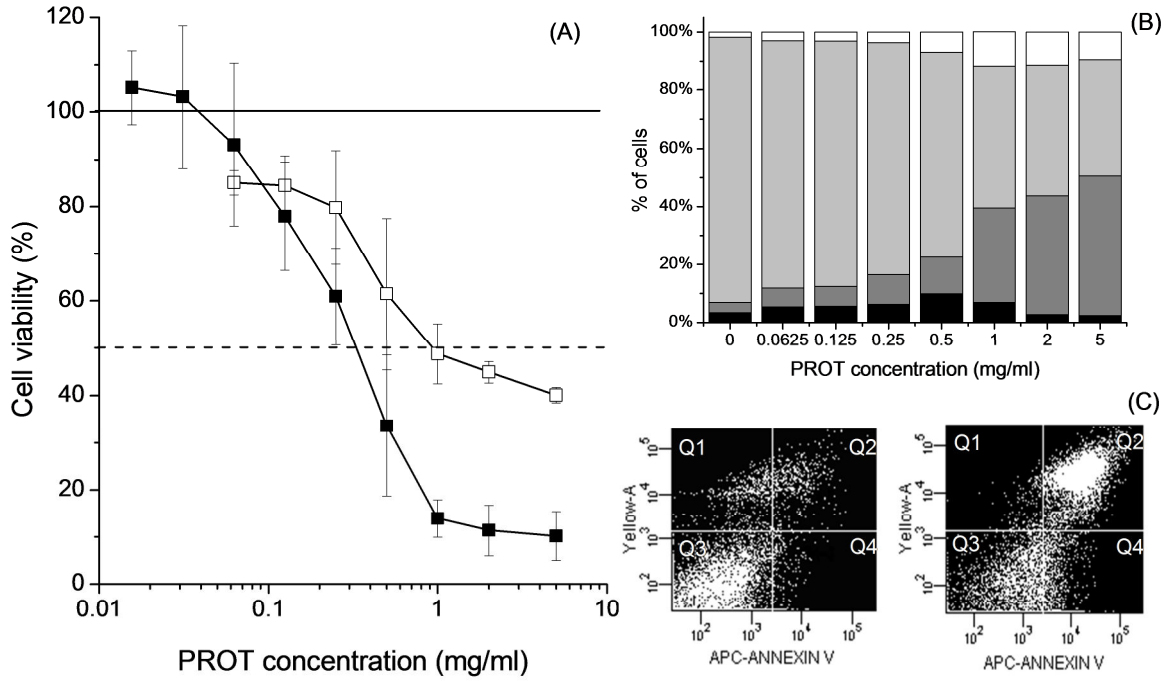

Figure 8. Cytotoxicity of protamine in Caco-2 cells after 72 h of exposure to protamine solution in medium: (A) Cell viability determined by flow cytometry (open squares) and MTS assay (filled squares) (mean ± S.D., n = 3); the dashed line indicates 50% cell viability. The viability of the control group was 100% (solid line). (B) Results of the apoptosis assay via flow cytometry (Q1 (black) and Q2 (dark grey) - late apoptosis and/or dead cell zone; Q3 (light grey) - living cell zone; Q4 (white) - cells in early apoptosis); the control (100% viability) was set in the sample of cells incubated with serum-free medium and analyzed without fluorescent dyes (Annexin V and PI). (C) Scatter plots of apoptosis assay: control (left) and PROT 5 mg/ml (right). Representative recordings of three similar experiments are presented. Q1, Q2, Q3 and Q4 are presented as described above.

Umerska et al., Self-assembled hyaluronate/protamine polyelectrolyte nanoplexes: Synthesis, stability, biocompatibility and potential use as peptide carriers, Figure 9

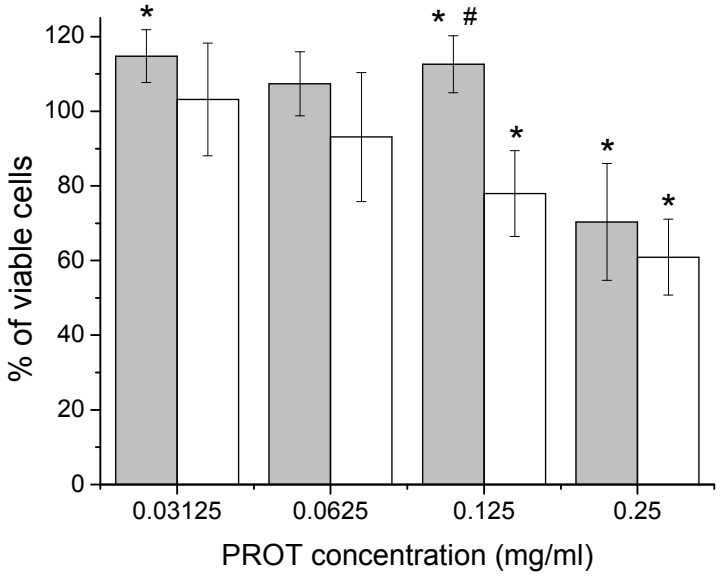

Figure 9. Viability of Caco-2 cells via MTS assay after 72 h of incubation with HA257/PROT NPs (HA/PROT MMR=3.1) and PROT (mean ± S.D., n = 3). Grey bars indicate NPs and open bars indicate PROT solution. * $p<0.05$ vs. control and # $p<0.05$ vs. PROT.

Umerska et al., Self-assembled hyaluronate/protamine polyelectrolyte nanoplexes: Synthesis, stability, biocompatibility and potential use as peptide carriers, graphical abstract